Published in final edited form as:
J Med Chem. 2013 March 28; 56(6): 2700–2704. doi:10.1021/jm400159c.

The Development of Highly Potent Inhibitors for Porcupine

Xiaolei Wang[†], **Jesung Moon**[‡], **Michael E. Dodge**[§], **Xinchao Pan**[¶], **Lishu Zhang**[§], **Jordan M. Hanson**[†], **Rubina Tuladhar**[§], **Zhiqiang Ma**[†], **Heping Shi**[†], **Noelle S. Williams**[†], **James F. Amatruda**[‡,¶], **Thomas J. Carroll**[¶], **Lawrence Lum**[§], and **Chuo Chen**[*,†]

[†]Department of Biochemistry, The University of Texas Southwestern Medical Center, 5323 Harry Hines Boulevard, Dallas, Texas 75390, United States

[‡]Department of Pediatrics, The University of Texas Southwestern Medical Center, 5323 Harry Hines Boulevard, Dallas, Texas 75390, United States

[§]Department of Cell Biology, The University of Texas Southwestern Medical Center, 5323 Harry Hines Boulevard, Dallas, Texas 75390, United States

[¶]Department of Internal Medicine and Molecular Biology, The University of Texas Southwestern Medical Center, 5323 Harry Hines Boulevard, Dallas, Texas 75390, United States

Abstract

Porcupine is a member of the membrane-bound O-acyltransferase family proteins. It catalyzes the palmitoylation of Wnt proteins, a process required for their secretion and activity. We recently disclosed a class of small molecules (IWPs) as the first reported Porcn inhibitors. We now describe the structure-activity relationship studies and the identification of sub-nanomolar inhibitors. We also report herein the effects of IWPs on Wnt-dependent developmental processes including zebrafish posterior axis formation and kidney tubule formation.

INTRODUCTION

The Wnt genes encode a large family of cell-to-cell signaling molecules that are essential to embryonic development and the regeneration of tissues. Aberrant Wnt signaling plays an important role in the formation and metastasis of tumors.[1] Currently, there is no drug targeting this cellular process in clinical use.[2] We recently identified a class of small molecules that inhibit the production of Wnt proteins and named them IWPs for Inhibitors of Wnt Production.[3] We further identified their molecular target to be Porcupine (Porcn), a membrane-bound O-acyltransferase (MBOAT) family protein.[4] This acyltransferase catalyzes the palmitoylation of Wnt to enable its exit from the secretory pathway and subsequent activation of cellular responses. Compromised Porcn activity commonly results in developmental disorders including focal dermal hypoplasia (Goltz syndrome) whereas hyperactivity of Porcn is associated with cancerous cell growth.[5] We envision that inhibition of Porcn will be an effective strategy for broadly suppressing Wnt signaling and thus hold potential in regenerative medicine and anti-cancer applications. Although genetically based targeting of Wnt signaling components suggests that chemical inhibitors of Wnt signaling may give rise to toxic effects, Porcn inhibitors have proven to be remarkably non-toxic in rodents.[6] Indeed, we surmise that these favorable results in preclinical tests were a pre-requisite to the Phase I trials underway for LGK974, a novel Porcn inhibitor.[2]

[*]Corresponding Author: Phone: 214-648-5048. chuo.chen@utsouthwestern.edu.

Supporting Information. Procedures for metabolic studies, metabolic profiles of IWP-L6 (**27**), and ^{1}H and ^{13}C NMR spectra of IWP-L6 (**27**). This material is available free of charge via the Internet at http://pubs.acs.org.

The four IWP molecules (**1**–**4**) identified in the initial screen of 200,000 compounds[7] bear similar molecular skeletons (Figure 1). They all suppress cell-autonomous Wnt signaling in mouse fibroblasts at nanomolar concentrations.[3] We consider the phthalazinone moiety of IWP-1 (**1**) and pyrimidinone moiety of IWP-2–4 (**2**–**4**) exchangeable scaffolding motifs. The benzothiazole moiety appears to be a conserved motif and the phenyl group tolerates both electronic and steric perturbations. Based on this information, we prepared an IWP-biotin conjugate and an IWP-Cy3 conjugate (**5**), and used them to demonstrate that IWP-2 (**2**) directly binds to Porcn.[3] We report herein the subsequent structure-activity relationship (SAR) studies yielding new Porcn inhibitors that suppress Wnt signaling at sub-nanomolar concentrations.

RESULTS AND DISCUSSION

We recently identified 13 additional Porcn inhibitors from the same screen that netted IWP-1–4 (**1**–**4**).[8] Five of them (**6**–**10**) possess similar molecular skeletons as IWP-1–4 (**1**–**4**) and provided further SAR information. The discovery of **6**–**10** as active Porcn inhibitors confirmed that the phthalazinone and pyrimidinone moieties are scaffolding motifs. Most importantly, the phenyl and benzothiazole groups of IWP-1–4 (**1**–**4**) can be replaced by an alkyl group and a simple aromatic group, respectively. We therefore hypothesized that IWPs bind to Porcn by fitting the phthalazinone/pyrimidinone and the benzothiazole regions into the binding pocket (Figure 2). Consistent with this model, we prepared **11** and **12** and found that they both failed to suppress the Wnt signaling at up to 25 μM in L-Wnt-STF cells, potentially due to reduced hydrophobic interactions. In addition, effective biotin and Cy3 conjugates (**5**) were obtained from derivatizing the phenyl group of IWP-2 (**2**), a region that is believed to be exposed to the solvent.

We started our investigation by examining effects of substituent groups on the benzothiazole and phenyl moieties (Table 1). As expected, there is no significant difference in potency for either the IWP-1 (**A**) or the IWP-2 (**B**) scaffolds harboring adducts to these moieties. Exchanging the substituent patterns observed in IWP-1–4 (**1**–**4**) (R^1=OMe or Me; R^2=H, *p*-F, *o*-OMe, or *p*-OMe) also did not significantly affect the activity, (entries 1–4). However, there is a steric preference at the 6-position of the benzothiazole. Removing the substituent group at the 6-position (R^1=H) of the benzothiazole led to drastic loss of activity (entry 5), presumably due to reduced interactions. Introducing a fluorine atom restored the activity (entry 6). Further increasing the size of the substituent group improved the activity (entries 7–11) but there is a limit of the size that can be tolerated (entry 12). Overall, these results support the hypothesis that the benzothiazole group fits into a binding pocket of Porcn. We therefore decided to focus on this region of the molecule for further SAR studies.

Motivated by the Porcn-inhibiting activities associated with **6**, **9**, and **10**, we replaced the benzothiazole group with other aromatic groups and examined the activity of molecules with general structure **C** (Figure 3). We first found that the benzothiazole group can be replaced by a quinoline group (**13**) despite compromised activity. We next found that the phenylthiazole derivatives (**14** and **15**) are also active Porcn inhibitors, and the 5-phenyl derivative **15** has a similar potency as IWP-2 (**2**). We subsequently found that weak or nearly no activity was observed with simple phenyl derivatives (**16**–**18**) that contain a small substituent group at the 4-position. However, installing a piperidine group resulted in an equal potent inhibitor (**19**) as IWP-2 (**2**). We therefore decided to explore the potential of biaryl systems as new Porcn inhibitors.

We first found that the 4-biphenyl derivative **20** was 40 times more potent than IWP-2 (**2**) while a significant loss of activity was observed with the 3- and 2-biphenyl derivatives (**21** and **22**). We next introduced a nitrogen atom to either the outer or inner phenyl ring (**23**–**27**).

We observed slight improvement of activity and with **24**, **26** and **27**, which are also more soluble than IWP-2 (**2**) and **20**. Introduction of an additional nitrogen atom (**28**–**30**) did not further improve the activity. We also attempted to replace the phenyl group with a furan or thiophene group (**32**–**37**) and found the 2-thiophenyl derivative **35** a highly potent Wnt inhibitor.

Among the five newly identified sub-nanomolar IWPs, we selected **27** for further biological evaluations and named **27** IWP-L6. We confirmed that IWP-L6 (**27**) effectively suppressed the phosphorylation of dishevelled 2 (Dvl2) in HEK293 cells, a biochemical event associated with many Wnt-dependent cellular responses (Figure 4).[8,9] We further profiled the in vivo stability of IWP-L6 (**27**) (Figure 5). Whereas IWP-L6 (**27**) was stable in human plasma over 24 h, it was rapidly metabolized in rat plasma ($t_{1/2}$ = 190 min), murine plasma ($t_{1/2}$ = 2 min), and the murine liver S9 fractions ($t_{1/2}$ = 26 min). The major metabolites are the amide cleavage products (see Supporting Information). Similar species-dependent metabolitic profiles due to the involvement of carboxylesterase (CES) have been reported with other drug candidates.[10,11] These observations are consistent with the elevated activity of CES in mouse and rat but not human.[12–14]

Despite its modest metabolic stability in mouse-derived plasma, IWP-L6 (**27**) was highly active in zebrafish. We had previously shown that both the tankyrase (Tnks) inhibitor IWR-1 and the Porcn inhibitor IWP-12 (**7**) effectively block the regeneration of the tailfin, a Wnt-dependent process, in adult and juvenile fish.[3,8,16] We herein show that IWP-L6 (**27**) exhibited more potent activity (Figure 6). We further show that IWP-L6 (**27**) and **35**, but not **30** and **32**, effectively inhibited posterior axis formation, a Wnt/β-catenin dependent developmental process, at low micromolar concentrations (Figure 7). IWP-L6 (**27**) and **35** are therefore at least 10 times more potent than IWP-12 (**7**) and 2.5 times more potent than IWR-1 in this in vivo assay.[16] While there is only 69% sequence identity between mouse Porcn and zebrafish Porcn, the in vitro EC_{50} values (Figure 3) measured in mouse fibroblasts (L cells) correlate with the in vivo activity observed in fish but not linearly.

We have previously shown that IWP2 (**2**) specifically and reversibly blocks Wnt signaling and Wnt mediated branching morphogenesis in cultured mouse embryonic kidneys.[8,17] We now show that IWP-L6 (**27**) is 100 times more potent than IWP-2 (**2**) in these experiments. We cultured embryonic day (E) 11.5 kidneys in media containing various doses (1 nM to 1 μM) of IWP-L6 (**27**). Doses of 10 nM and above significantly reduced branching morphogenesis relative to DMSO treated controls (Figure 8). Doses of 50 nM and above completely blocked branching morphogenesis indicating a complete inhibition of Wnt signaling. In comparison, a dose of 5 μM of IWP-2 (**2**) was required to obtain similar results.[8,17]

CONCLUSION

The SAR data presented herein suggest that two structural motifs of IWPs interact with Porcn and are important for the activity. We further showed that optimization of one of these motifs led to a significant improvement in activity. The newly discovered IWP-L6 (**27**) is a sub-nanomolar Porcn inhibitor. It has good stability in human plasma but compromised stability in rat and mouse plasma. The in vivo activities of IWP-L6 (**27**) were also validated by their ability to disrupt well-established Wnt-dependent developmental processes of embryonic and juvenile zebrafish, and the branching morphogenesis in cultured mouse embryonic kidneys. Further tuning of its activity and stability is underway.

EXPERIMENTAL SECTION

General

All chemical reactions were performed in glassware under a positive pressure of argon. The normal-phase flash column chromatography was performed with EMD silica gel 60 (230–400 mesh ASTM). TLC analyses were performed on EMD 250 μm Silica Gel 60 F_{254} plates and visualized by quenching of UV fluorescence (λ_{max}= 254 nm), or by staining ceric ammonium molybdate. ^{1}H and ^{13}C NMR spectra were recorded on Varian Inova-400. Chemical shifts for ^{1}H and ^{13}C NMR spectra are reported in ppm (δ) relative to the ^{1}H and ^{13}C signals in the solvent ($CDCl_3$: δ 7.26, 77.16 ppm; DMSO-*d*6: δ 2.50, 39.52 ppm) and the multiplicities are presented as follows: s = singlet, d = doublet, t = triplet, m = multiplet. Mass spectra were acquired on Agilent 6120 Single Quadrupole LC/MS. Analytic HPLC was performed using an Eclipse XDB-C18 5 μm column with dimension 4.6×150 mm using an Alltech 3300 evaporative light scattering detector. The purity of all compounds for biologically assays was determined to be >95% by HPLC.

Synthesis of IWP-L6 (27)

To a solution of 1,8-diazabicyclo[5.4.0]undec-7-ene (DBU, 26 mL, 0.17 mol) in methanol (90 mL) were added methyl thioglycolate (14.4 mL, 0.158 mol) and acrylonitrile (12 mL, 0.17 mol) at 0 °C. The solution was stirred at 0 °C for 5 h and then at 80 °C overnight. After cooling to room temperature, the solvent was evaporated, quenched with a saturated solution of ammonium chloride, and extracted with ethyl acetate. The organic layer was dried over sodium sulfate, concentrated, and purified by silica gel column chromatography (40% ethyl acetate/hexanes) to give 3-amino-2-(methoxycarbonyl)4,5-dihydrothiophene (9.72 g, 39%) as a yellow solid: ^{1}H NMR (400 MHz, $CDCl_3$) δ 2.86 (t, *J* = 8.0 Hz, 2H), 3.03 (t, *J* = 8.0 Hz, 2H), 3.68 (s, 3H).[18]

A solution of 3-amino-2-(methoxycarbonyl)4,5-dihydrothiophene (1.00 g, 5.78 mmol) and phenyl isothiocyanate (937 mg, 6.94 mmol) in pyridine (18 mL) was stirred at 100 °C overnight. The solvent was then evaporated and the residue was purified by silica gel column chromatography (30% ethyl acetate/hexanes then acetone) and then washed three times with ethyl acetate to give pure 3-phenyl-6,7-dihydrothieno[3,2-*d*]pyrimidine-2-thione-4-one (635 mg, 42%). ^{1}H NMR (400 MHz, DMSO-d_6) δ 13.17 (s, 1H) 7.30–7.50 (m, 3H), 7.08–7.20 (m, 2H), 3.20–3.40 (m, 4H).

To a solution of 5-phenylpyridin-2-amine (170 mg, 1.00 mmol) in benzene/THF (9/1, 10.0 mL) was added a solution of chloroacetylchloride (0.111 mL, 1.40 mmol) in benzene (1.0 mL). The reaction mixture was then stirred at 50 °C overnight. After cooling to room temperature, the solution was washed with a saturated solution of sodium bicarbonate and water, dried over sodium sulfate, and concentrated to give 2-chloro-*N*-(5-phenylpyridin-2-yl)acetamide, which was used directly for next step without purification.

A solution of 3-phenyl-6,7-dihydrothieno[3,2-*d*]pyrimidine-2-thione-4-one (81 mg, 0.310 mmol), 2-chloro-*N*-(5-phenylpyridin-2-yl)acetamide (80 mg, 0.325 mmol), and triethylamine (0.13 mL, 0.93 mmol) in *N*,*N*-dimethylformamide (DMF, 3.0 mL) was stirred at 80 °C for 2 h. The reaction was quenched with water, extracted with ethyl acetate, washed three times each with water and brine, dried over sodium sulfate, concentrated, and purified by silica gel column chromatography (30% ethyl acetate/hexanes) to give IWP-L6 (**27**) (136 mg, 93%) as white solid ^{1}H NMR (400 MHz, $CDCl_3$) 10.06 (s, 1H), 8.57 (d, *J* = 2.1 Hz, 1H), 8.25 (d, *J* = 8.6 Hz, 1H), 7.95 (dd, *J* = 8.6, 2.4 Hz, 1H), 7.56–7.63 (m, 5H), 7.48–7.56 (m, 2H), 7.40–7.47 (m, 1H), 7.29–7.35 (m, 2H), 3.85 (s, 2H), 3.54–3.62 (m, 2H), 3.44–3.52 (m, 2H); ^{13}C NMR (100 MHz, $CDCl_3$) δ 166.6, 160.2, 159.2, 157.4, 150.5, 146.3, 137.4,

136.7, 135.0, 133.0, 130.6, 130.0, 129.1, 128.6, 127.9, 126.8, 122.3, 113.7, 37.6, 37.0, 29.3. MS(ES)$^+$ calcd for $C_{25}H_{21}N_4O_2S_2$ $(M+H)^+$ 473.1, found 473.1.

Supplementary Material

Refer to Web version on PubMed Central for supplementary material.

Acknowledgments

Financial support was provided by the Cancer Prevention and Research Institute of Texas (RP100119 to L.L. and C.C.), National Institute of Health (5R21HD061303 to J.F.A., C.C., and L.L., R01CA135731 to J.F.A., and R01DK080004 & P30DK079328 to T.C.), the Welch Foundation (I-1596 to C.C., and I-1665 to L.L.), and UT Southwestern. L.L. is a Virginia Murchison Linthicum Scholar in Medical Research, and C.C. is a Southwestern Medical Foundation Scholar in Biomedical Research. X.P. is supported by a postdoctoral fellowship from the National Kidney Foundation (FLB1686).

ABBREVIATIONS

CES	carboxylesterase
Dvl2	dishevelled 2
MBOAT	membrane-bound O-acyltransferase
Porcn	Porcupine
SAR	structure-activity relationship
Tnks	tankyrase

References

1. Clevers H, Nusse R. Wnt/β-Catenin Signaling and Disease. Cell. 2012; 149:1192–1205. [PubMed: 22682243]
2. Lum L, Clevers H. The Unusual Case of Porcupine. Science. 2012; 337:922–923. [PubMed: 22923569]
3. Chen B, Dodge ME, Tang W, Lu J, Ma Z, Fan CW, Wei S, Hao W, Kilgore JA, Williams NS, Roth MG, Amatruda JF, Chen C, Lum L. Small Molecule-mediated Disruption of Wnt-dependent Signal Transduction in Tissue Regeneration and Cancer. Nat Chem Biol. 2009; 5:100–107. [PubMed: 19125156]
4. Yang J, Brown MS, Liang G, Grishin NV, Goldstein JL. Identification of the acyltransferase that octanoylates ghrelin, an appetitestimulating peptide hormone. Cell. 2008; 132:387–396. [PubMed: 18267071]
5. Chen Z, Li J, Li QS, Fan JQ, Dong XM, Xu JP, Wang XM, Yang GW, Yan P, Wen GZ, Zhang YT, Niu RG, Nan PH, He J, Zhou HM. Suppression of PPN/MG61 Attenuates Wnt/β-Catenin Signaling Pathway Induces Apoptosis in Human Lung Cancer. Oncogene. 2008; 27:3483–3488. [PubMed: 18193088]
6. Proffitt KD, Madan B, Ke Z, Pendharkar V, Ding L, Lee MA, Hannoush RN, Virshup DM. Pharmacological Inhibition of the Wnt Acyltransferase PORCN Prevents Growth of WNT-Driven Mammary Cancer. Cancer Res. 2013; 73:502–507. [PubMed: 23188502]
7. Compounds in the UTSW library were purchased from ChemDiv (100,000), ChemBridge (75,500), ComGenex (22,000), Prestwick (1,100), and TimTek (500). Compounds were selected for being able to pass 48 structure-based filters that identified undesirable characteristics as well as for satisfying a relaxed set of Lipinski's' rules for good bioavailability.
8. Dodge ME, Moon J, Tuladhar R, Lu J, Jacob LS, Zhang L-s, Shi H, Wang X, Moro E, Mongera A, Argenton F, Karner CM, Carroll TJ, Chen C, Amatruda JF, Lum L. Diverse Chemical Scaffolds Support Direct Inhibition of the Membrane Bound O-Acyltransferase Porcupine. J Biol Chem. 2012; 287:23246–23254. [PubMed: 22593577]

9. Jacob LS, Wu X, Dodge ME, Fan C-W, Kulak O, Chen B, Tang W, Wang B, Amatruda JF, Lum L. Genome-Wide RNAi Screen Reveals Disease-Associated Genes That Are Common to Hedgehog and Wnt Signaling. Sci Signal. 2011; 4:ra4. [PubMed: 21266715]
10. Eng H, Niosi M, McDonald TS, Wolford A, Chen Y, Simila STM, Bauman JN, Warmus J, Kalgutkar AS. Utility of the Carboxylesterase Inhibitor Bis-para-nitrophenylphosphate (BNPP) in the Plasma Unbound Fraction Determination for a Hydrolytically Unstable Amide Derivative and Agonist of the TGR5 Receptor. Xenobiotica. 2010; 40:369–380. [PubMed: 20297923]
11. Liu L, Halladay JS, Shin Y, Wong S, Coraggio M, La H, Baumgardner M, Le H, Gopaul S, Boggs J, Kuebler P, Davis JC Jr, Liao XC, Lubach JW, Deese A, Sowell CG, Currie KS, Young WB, Khojasteh SC, Hop CECA, Wong H. Significant Species Difference in Amide Hydrolysis of GDC-0834, a Novel Potent and Selective Bruton's Tyrosine Kinase Inhibitor. Drug Metab Dispos. 2011; 39:1840–1849. [PubMed: 21742900]
12. Berry LM, Wollenberg L, Zhao Z. Esterase Activities in the Blood, Liver and Intestine of Several Preclinical Species and Humans. Drug Metab Lett. 2009; 3:70–77. [PubMed: 19601867]
13. Rudakova EV, Boltneva NP, Makhaeva GF. Comparative Analysis of Esterase Activities of Human, Mouse, and Rat Blood. Bull Exp Biol Med. 2011; 152:73–75. [PubMed: 22803044]
14. Bahar FG, Ohura K, Ogihara T, Imai T. Species Difference of Esterase Expression and Hydrolase Activity in Plasma. J Pharm Sci. 2012; 101:3979–3988. [PubMed: 22833171]
15. Moro E, Ozhan-Kizil G, Mongera A, Beis D, Wierzbicki C, Young RM, Bournele D, Domenichini A, Valdivia LE, Lum L, Chen C, Amatruda JF, Tiso N, Weidinger G, Argenton F. *In Vivo* Wnt Signaling Tracing through a Transgenic Biosensor Fish Reveals Novel Activity Domains. Dev Biol. 2012; 366:327–340. [PubMed: 22546689]
16. Lu J, Ma Z, Hsieh JC, Fan CW, Chen B, Longgood JC, Williams NS, Amatruda JF, Lum L, Chen C. Structure/Activity Relationship Studies of Small-Molecule Inhibitors of Wnt Response. Bioorg Med Chem Lett. 2009; 19:3825–3827. [PubMed: 19410457]
17. Karner CM, Michael Dodge CE, Ma Z, Lu J, Chen C, Lum L, Carroll TJ. Tankyrase Is Necessary for Canonical Wnt Signaling during Kidney Development. Dev Dyn. 2010; 239:2014–2023. [PubMed: 20549720]
18. Baraldi PG, Cacciari B, Manfredini S, Pollini GP, Simoni D, Spalluto G, Zanirato V. Unusual Ring-Opening Reaction of 6,7-Dihydrothieno[3,2-*d*]pyrimidine-2,4-dione Derivatives Leading to 5-(Alkylthio)-6-vinyluracils. J Org Chem. 1995; 60:1461–1463.

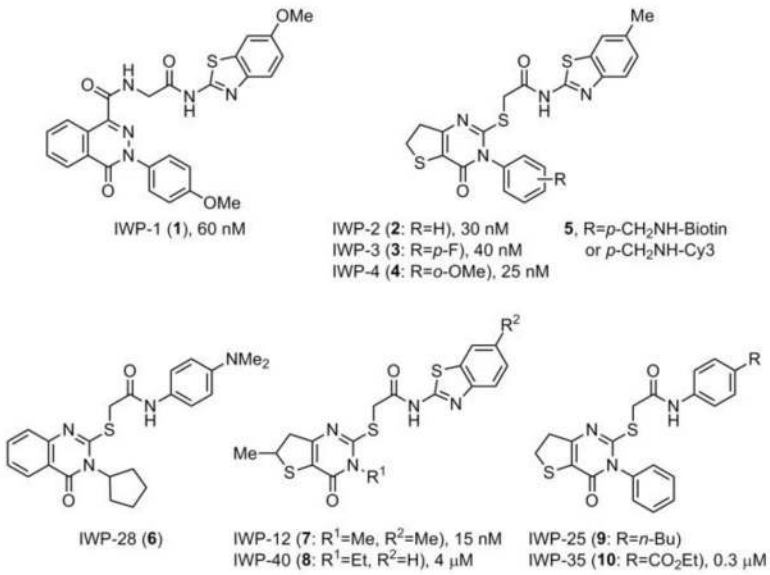

Figure 1.
The structures and activities of IWPs identified from a high-throughput screen in cells exhibiting cell-autonomous Wnt signaling.

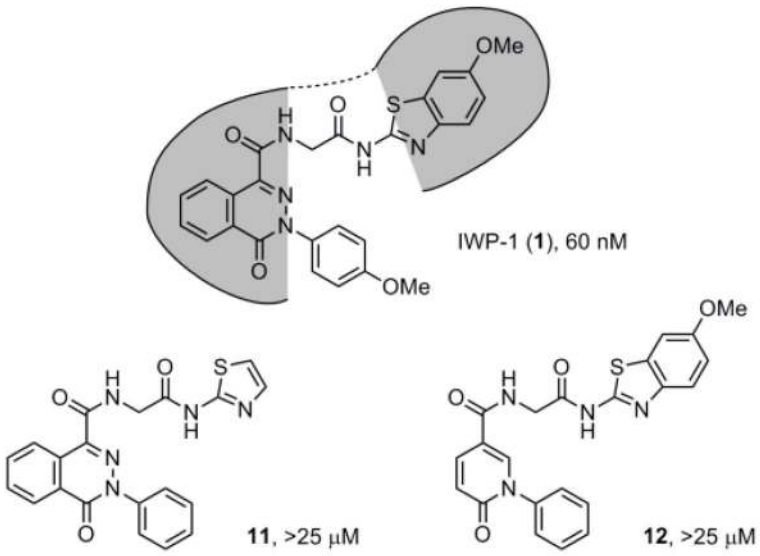

Figure 2.
The phthalazinone/pyrimidinone and the benzothiazole moieties of IWPs are important for their binding to Porcn.

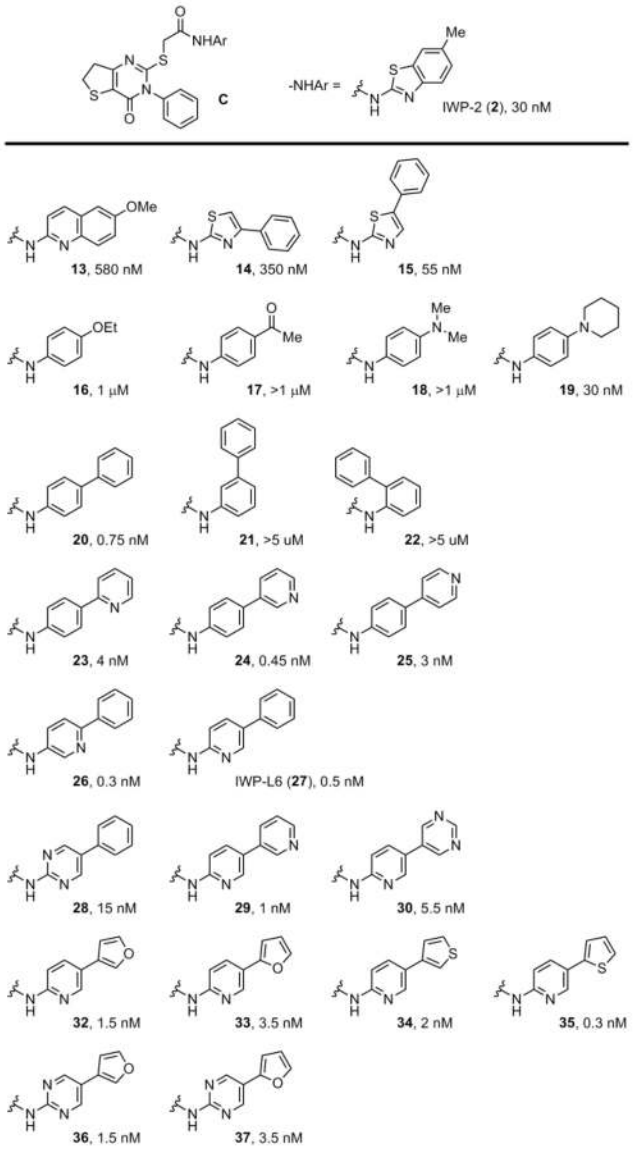

Figure 3.
Effects of the arylamide groups on the Porcn-inhibiting activity.

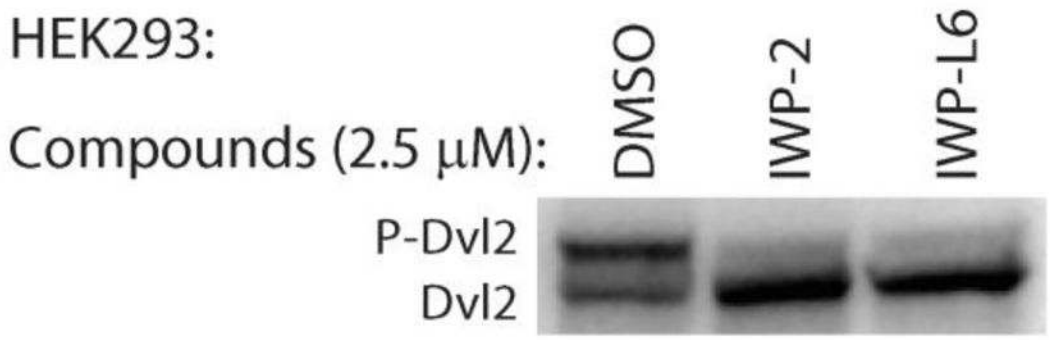

Figure 4.
IWP-L6 (**27**) blocks the phosphorylation of the cytoplasmic Wnt pathway effector Dvl2.

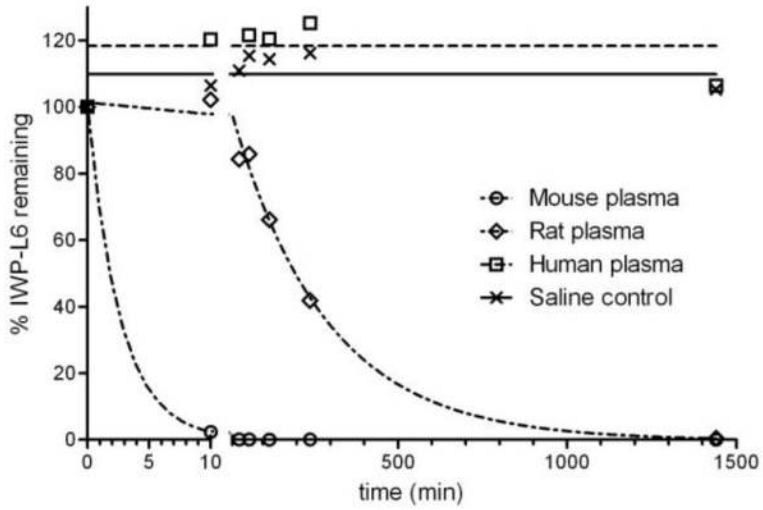

Figure 5.
Stability of IWP-L6 (**27**) in plasma.

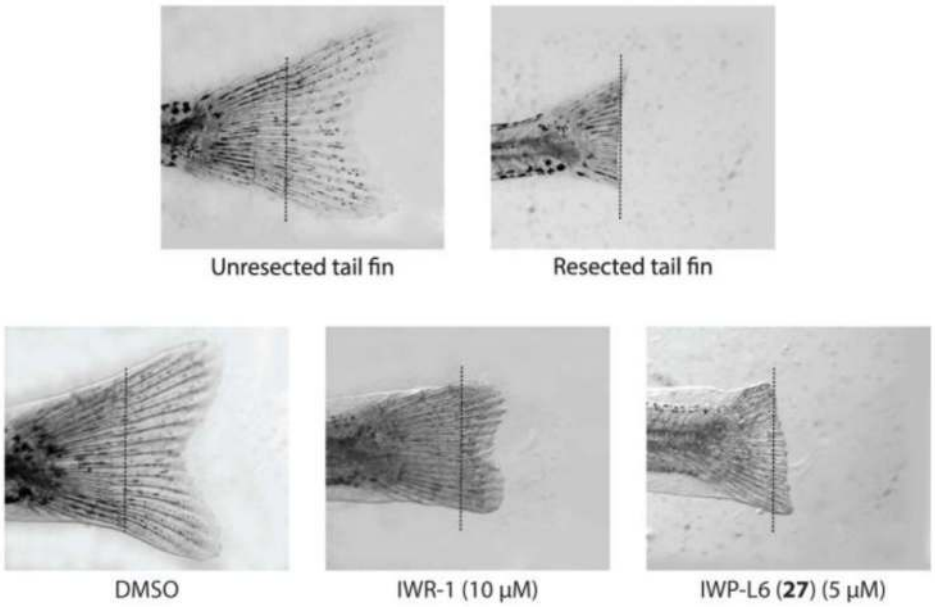

Figure 6.
Inhibition of the regeneration of tailfin of juvenile zebrafish.

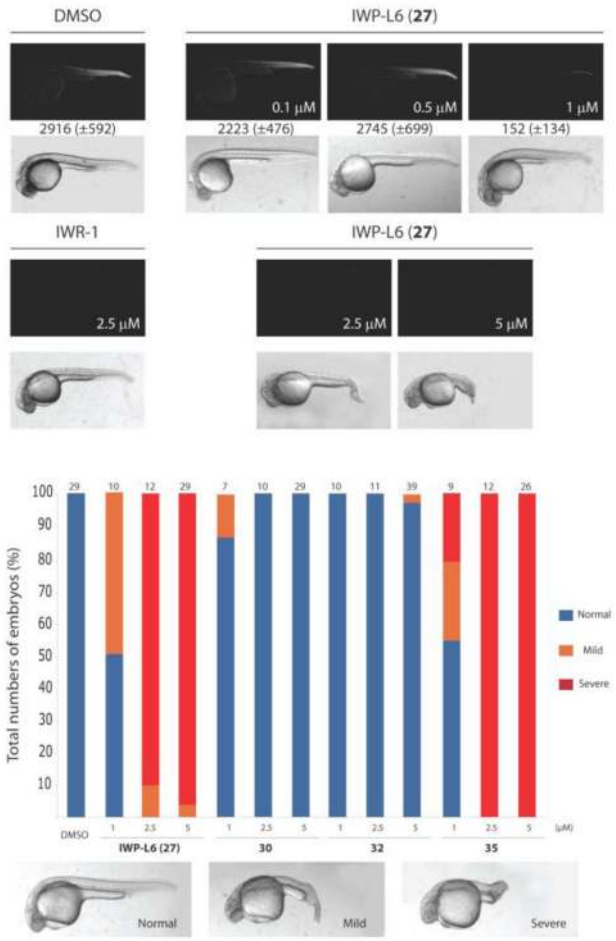

Figure 7.

IWP-L6 (**27**) inhibits posterior axis formation. Zebrafish embryos harboring an mCherry-based reporter of Wnt/β-catenin signaling[15] were treated with increasing concentrations of IWP-L6 (**27**) in the aquarium water (top). Fluorescence intensity of animals was quantified as before.[8] Activity of the IWP compounds IWP-L6 (**27**), **30**, **32**, and **35** was measured using the posterior axis formation assay (bottom).

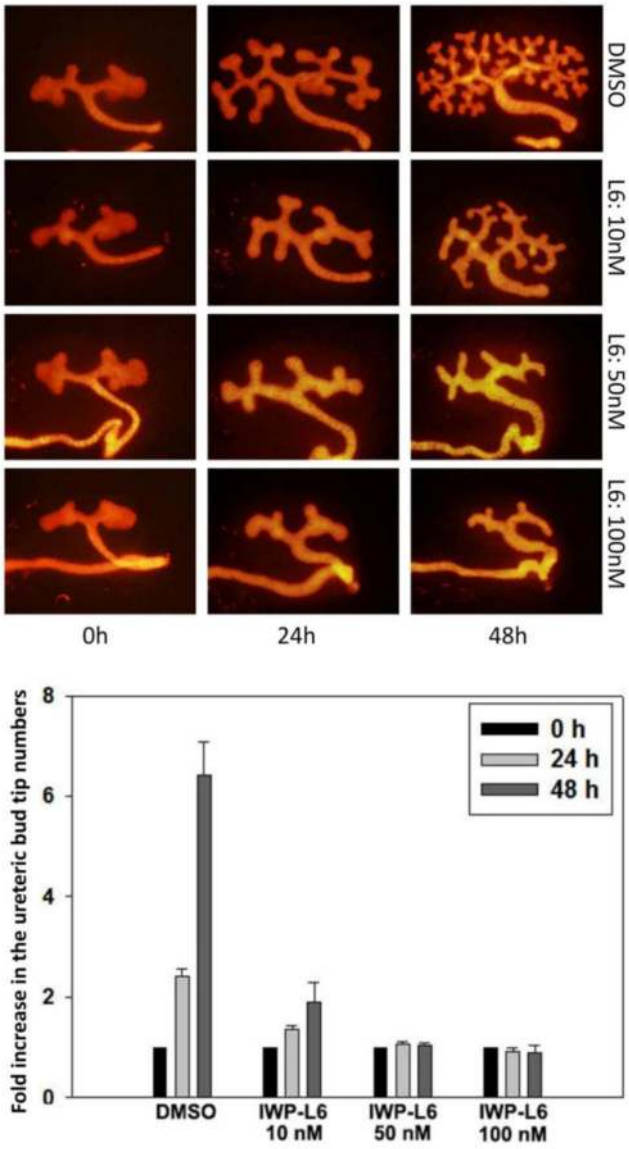

Figure 8.

IWP-L6 (**27**) inhibits Wnt mediated branching morphogenesis in cultured embryonic kidneys. Hoxb7Cre;RosaTomato kidneys were dissected from E11.5 embryos and cultured at the air/media interface (top).[8,17] Media was replaced every 24 hours. Images were captured every 24 hours using a Zeiss Lumar V12 fluorescent stereoscope. Magnitude: 80× at 0 h and 24 h; 60× at 48h. The fold increase in the number of ureteric bud tips between time=0 and 48 hours for each treatment was quantified (bottom). Statistics were performed using Student T-test.

Table 1

Effects of the substituent groups of the phenyl and benzothiazole groups of IWP-1 (1) and IWP-2 (2)[a]

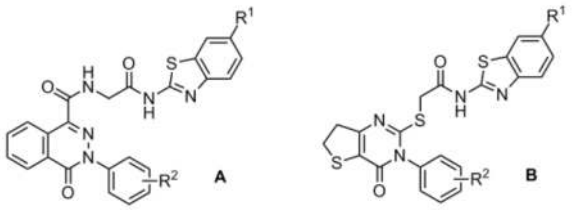

Entry	R^1	Scaffold	R^2			
			H	*p*-F	*o*-OMe	*p*-OMe
1	OMe	**A**	210	90	90	60
2		**B**	40	250	50	120
3	Me	**A**	35	100		25
4		**B**	30	40	30	
5	H	**A**	2600	>25000	10000	25000
6	F	**A**	470			
7	Cl	**A**	30	25		15
8		**B**	40	175	50	35
9	CF_3	**A**	110	90		
10		**B**	40	100	30	100
11	NO_2	**A**	240			
12	COOEt	**A**	>25000			

[a] EC_{50} values in nM.